

Supporting Information (SI)

Multi-stimuli Responsive Carbazole based Low Molecular Weight Gelator: Nanomolar Sensing of Cyanide Ions and Electrochromic Switching in Real-time

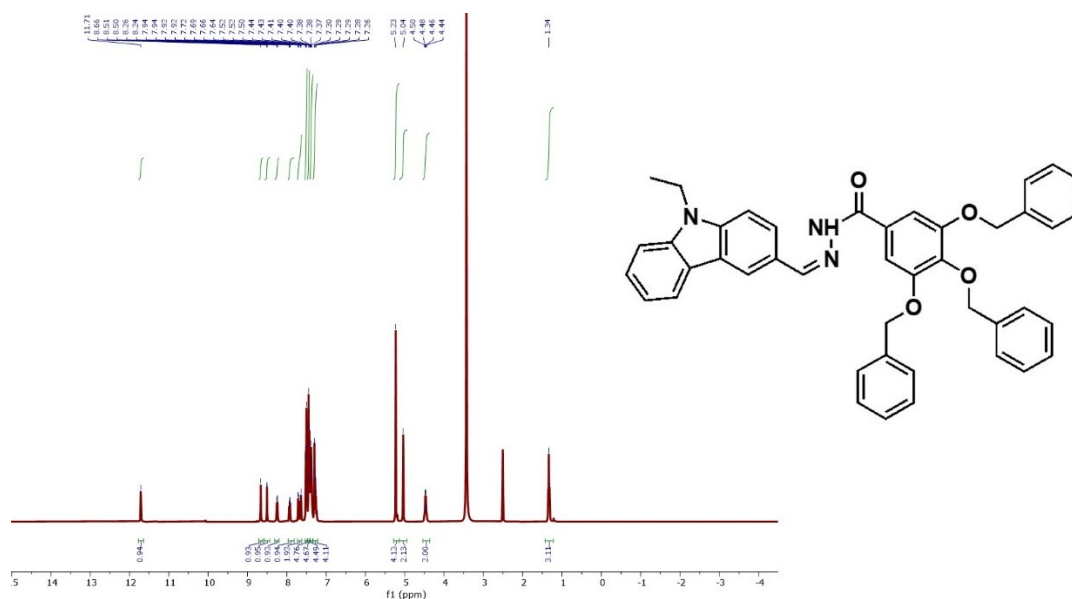
Celin Rooth, Swatilekha Pratihari, Yuvaraj Palani, Anandhakumar Sukeri, Edamana Prasad

Department of Chemistry, Indian Institute of Technology Madras (IITM), Chennai 600036, India

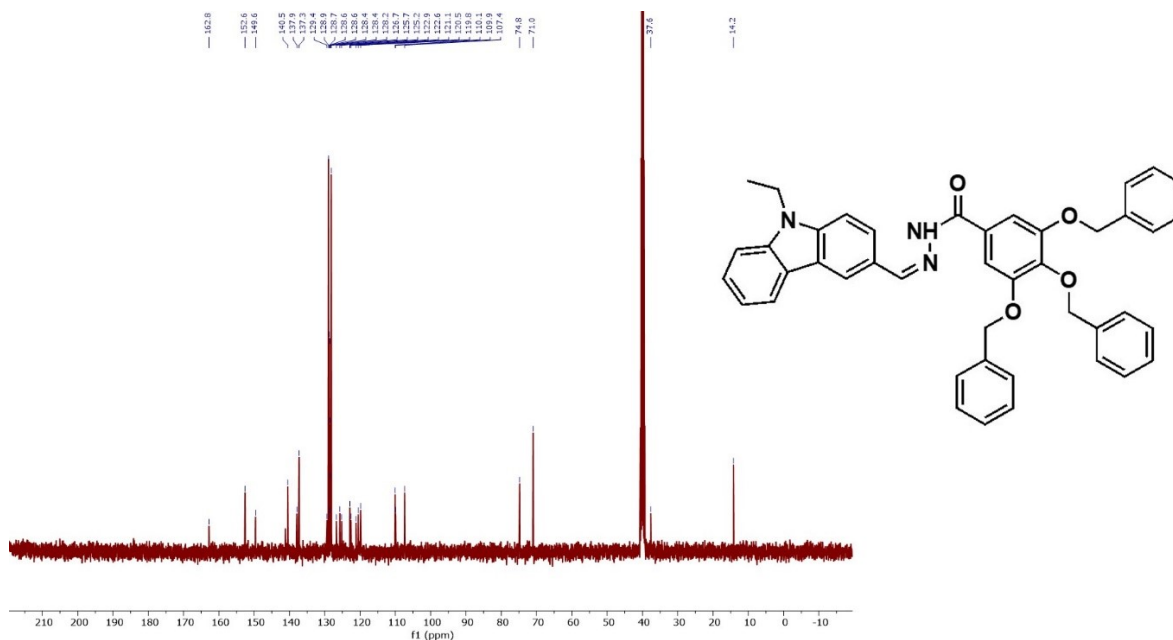
Table of contents

Figure SI-1: ^1H NMR spectrum of CBG in DMSO- d_6	2
Figure SI-2: ^{13}C NMR spectrum of CBG in DMSO- d_6	2
Figure SI-3: HRMS of CBG.....	3
Figure SI-4: Lippert-Mataga plot.....	3
Figure SI-5: DFT Calculated FMOs of CBG	3,4
Figure SI-6: DLS traces of CBG in THF/ H_2O mixtures at different water fractions.....	4
Figure SI-7: SEM images of aggregates at lower water fractions.....	5
Figure SI-8: DLS traces at two different scattering angles and its SEM image.....	6
Figure SI-9: CBG gel in Dioxane- H_2O mixture.....	6
Figure SI-10: FT-IR spectra of CBG in its gel, solution and solid state.....	7
Figure SI-11: Absorption spectra changes upon addition of various anions	8
Figure SI-12: Stern-Volmer plot and determination of detection limit of CBG for CN^- sensing.....	8
Figure SI-13: Sensing studies in solid and gel state.....	9
Figure SI-14: SEM image of CBG gel before and after addition of CN^-	9
Figure SI-15: Sensing of CN^- in real water sample.....	10
Figure SI-16: Yellow colour of the solution that appeared at 1.7 V.....	12
Figure SI-17: CV obtained when FTO plate is used as the working electrode.....	12
Figure SI-18: CBG gel sandwiched between FTO plates and CV in gel state.....	12
Table SI-1: Table containing the details of gelation test.....	7
Table SI-2: Comparison table of literature reports of cyanide sensing.....	11
Scheme SI-1: Deprotonation followed by the resonance stabilization.....	7

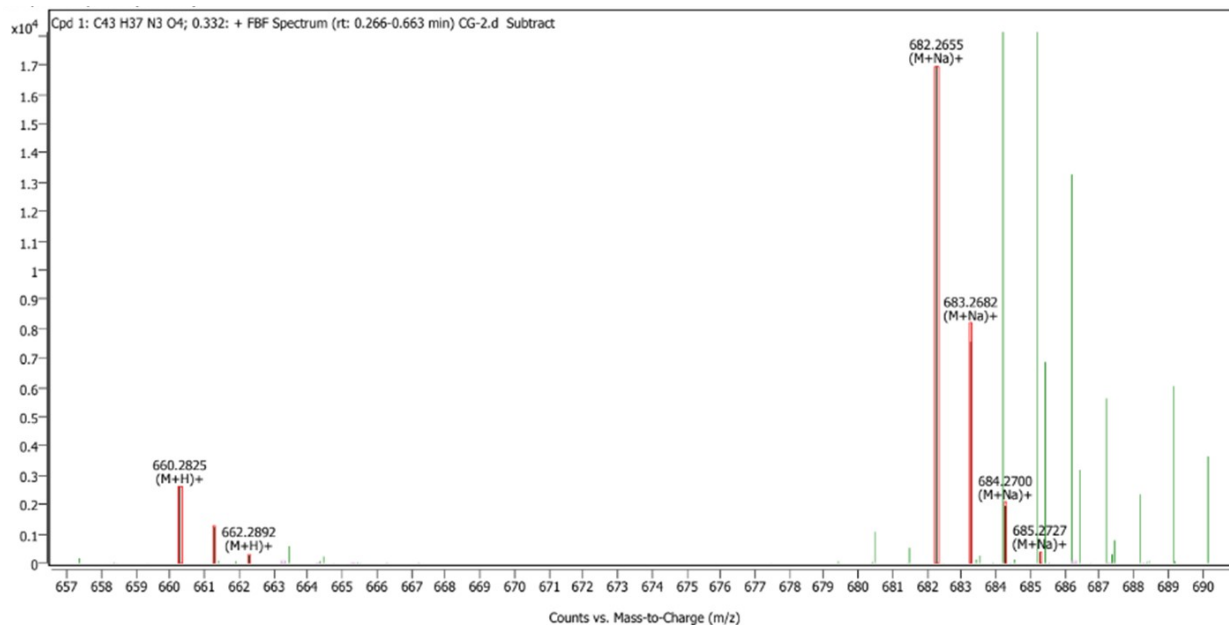
¹H NMR Spectrum

Figure SI-1. ¹H NMR spectrum of CBG in DMSO-d₆.

¹³C NMR Spectrum



HRMS



Compound ID Table

Cpd	Formula	Mass (Tgt)	Calc. Mass	Mass	Species	Diff(Tgt.ppm)	mDa
1	C43 H37 N3 O4	659.2784	659.2759	660.2825 682.2655	(M+H)+ (M+Na)+	-3.86	-2.54

Figure SI-3. HRMS of CBG.

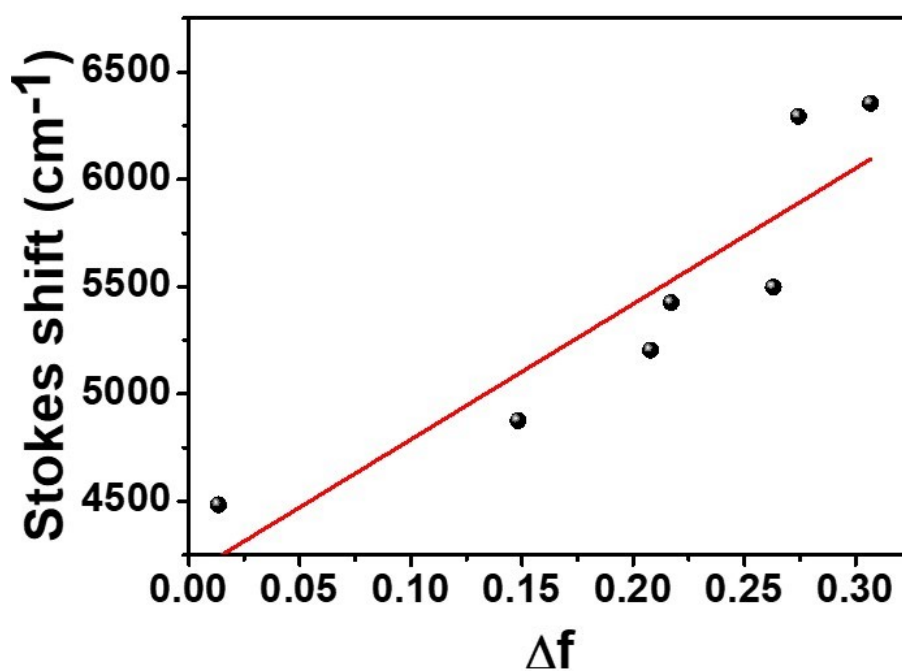


Figure SI-4. Lippert-Mataga plot of CBG.

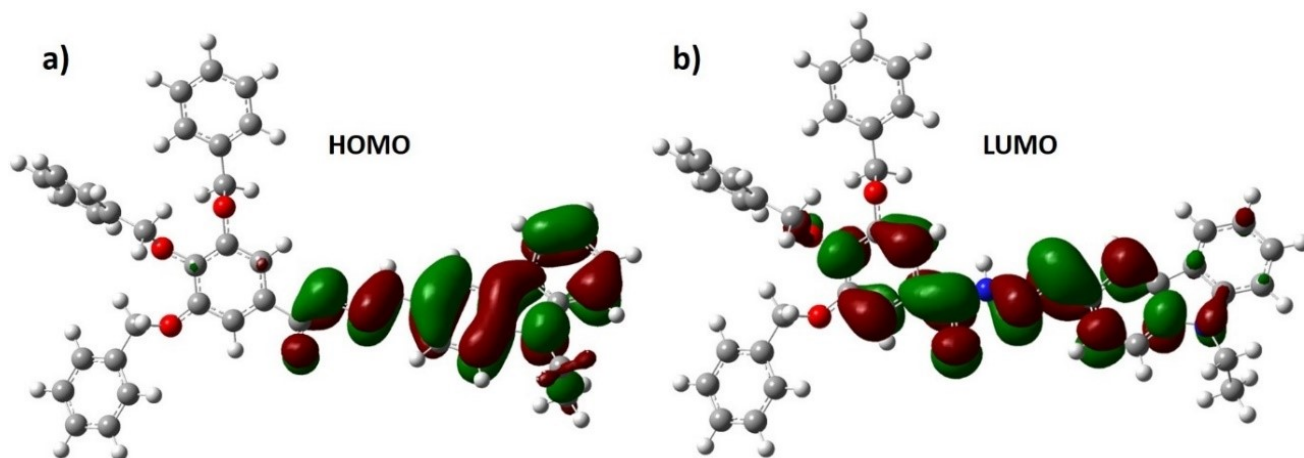


Figure SI-5. a) HOMO and b) LUMO orbitals in the optimized ground-state structure of CBG.

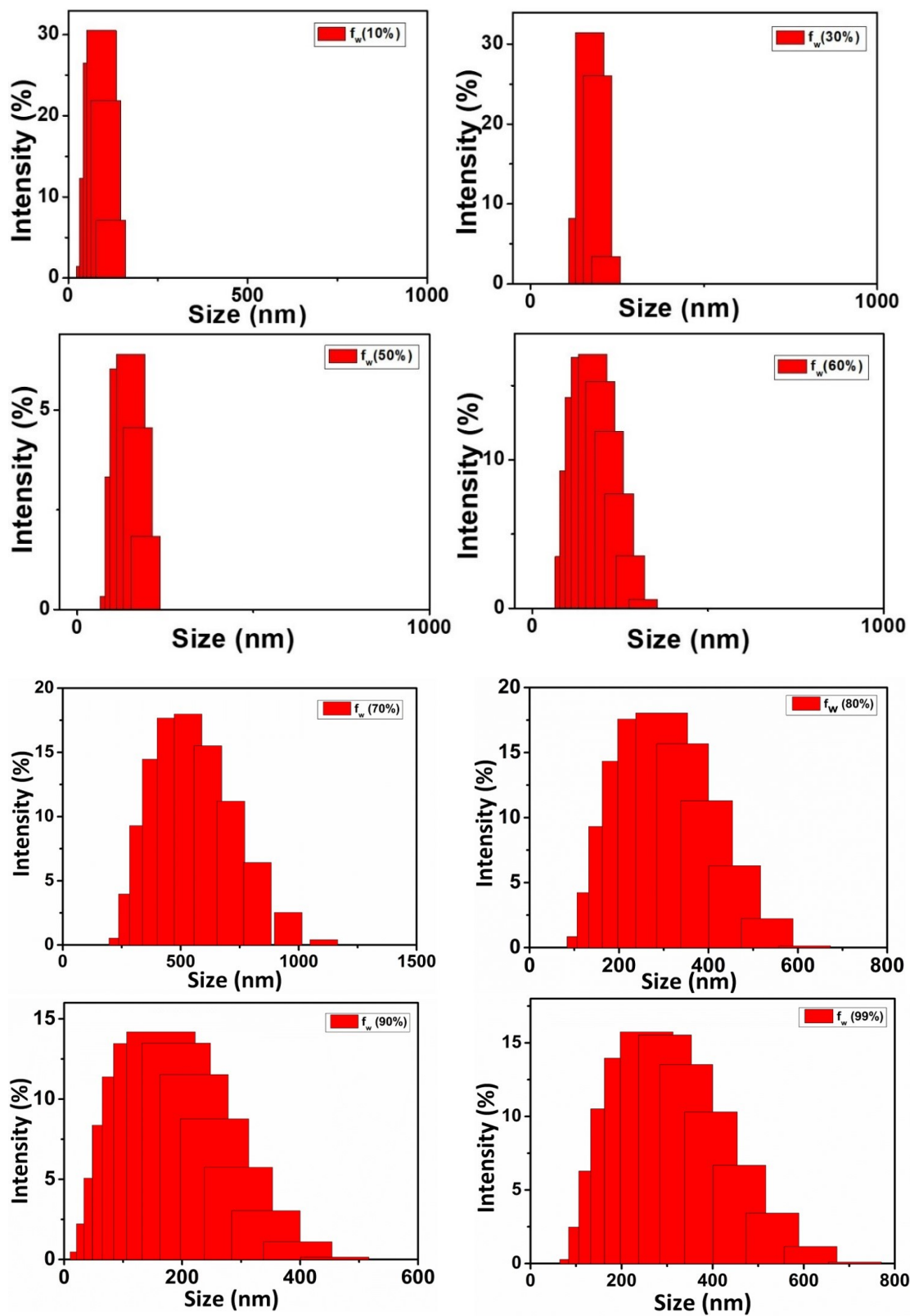


Figure SI-6. DLS traces of CBG in THF/H₂O mixtures at $f_w = 10\%$, 30% , 50% , 60% , 70% , 80% , 90% , 99% .

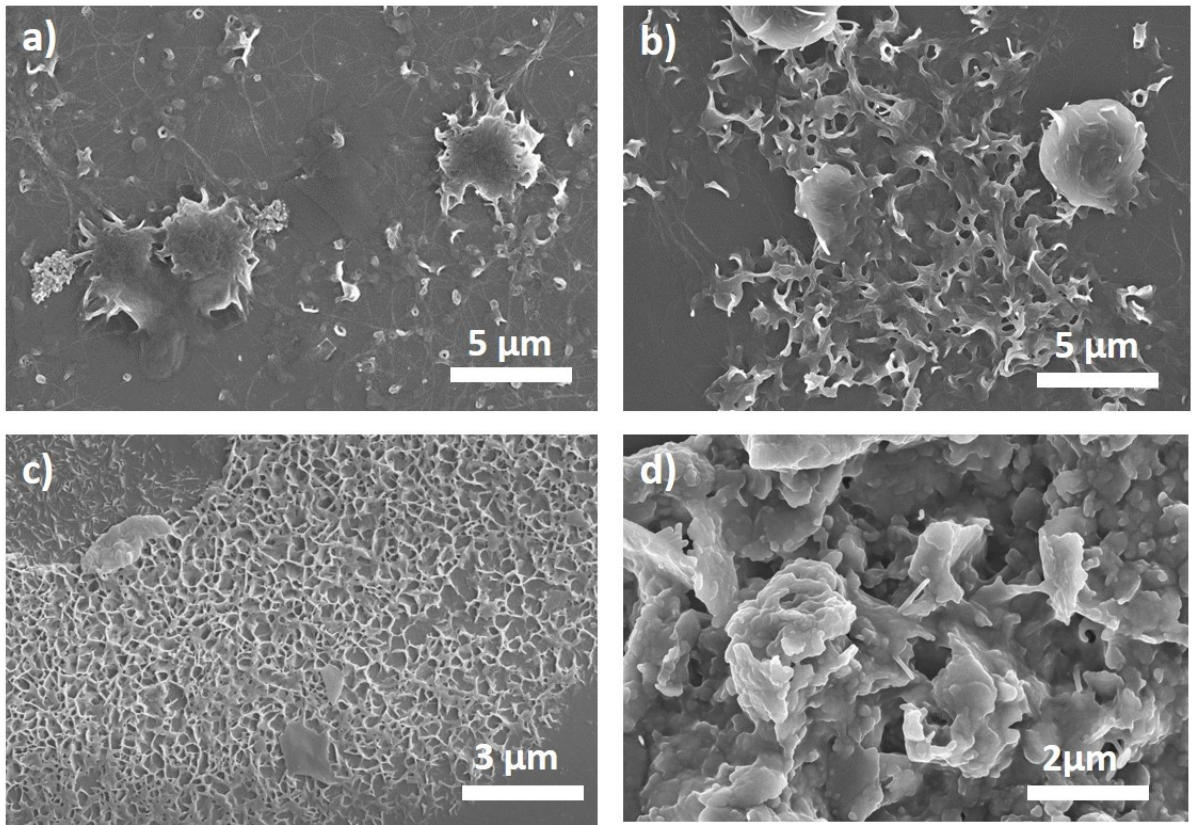


Figure SI-7. SEM images of a) 10%, b) 30%, c) 50%, d) 60% water fractions

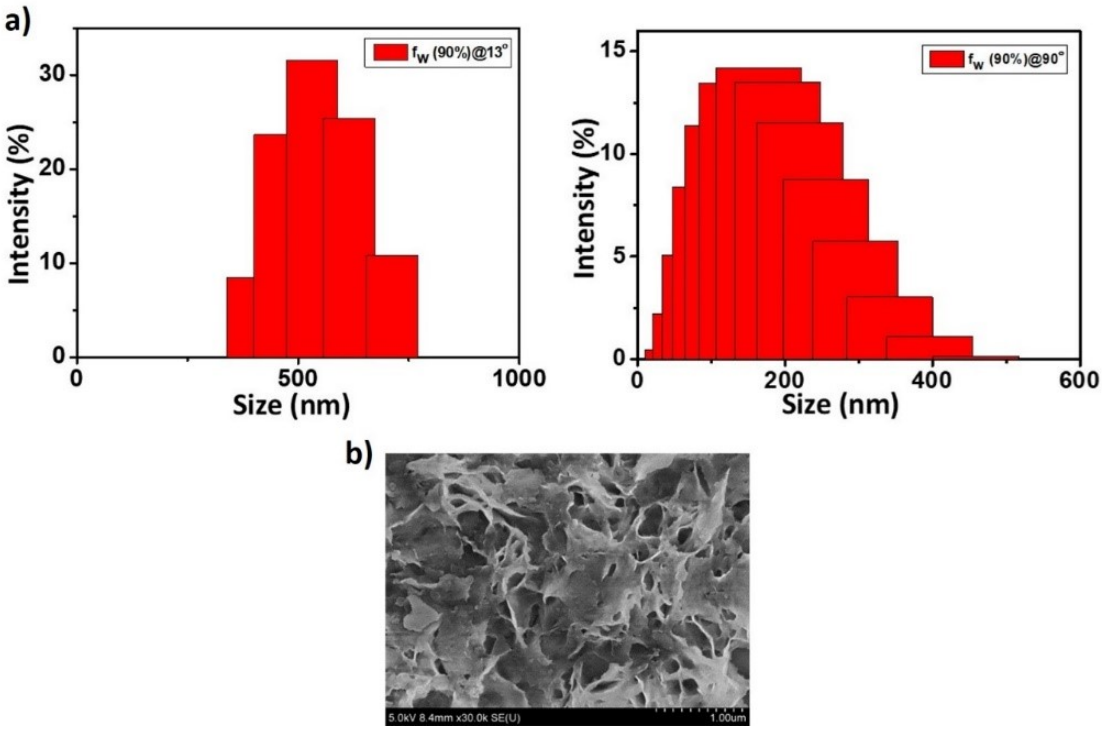


Figure SI-8. a) DLS traces of CBG ($f_w=90%$) in THF/H₂O mixtures at two different scattering angles (13°, 90°) and b) SEM image of $f_w=90%$ (90:10).

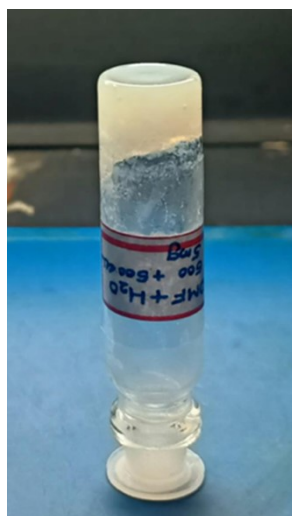


Figure SI-9. CBG gel in Dioxane-H₂O mixture.

Entry	Solvent	Phase (CGC)
1	CHCl ₃	S
2	DCM	S
3	THF	S
4	DMSO	S
5	DMF	S
6	Dioxane	S
7	ACN	I
8	Hexane	I
9	DMF-H ₂ O (1:1)	G (5 mg)
10	Dioxane-H ₂ O (1:1)	G (5 mg)

Table SI-1. Table containing the details of gelation test.

(S: soluble, I: Insoluble G: gel formed)

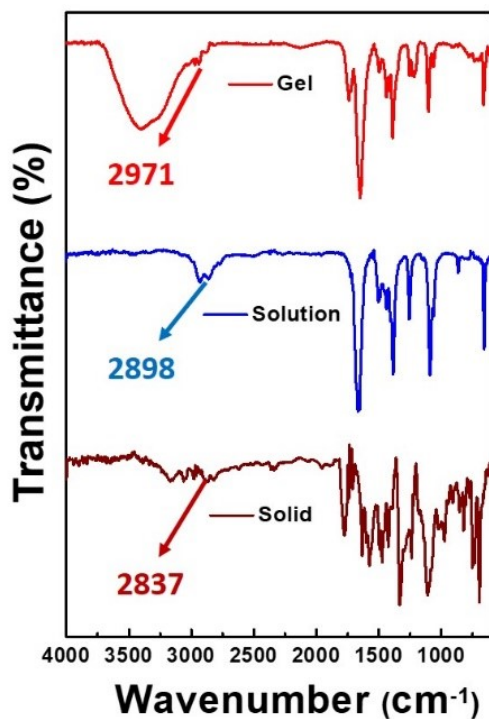


Figure SI-10. FT-IR spectra of CBG in its gel, solution and solid state

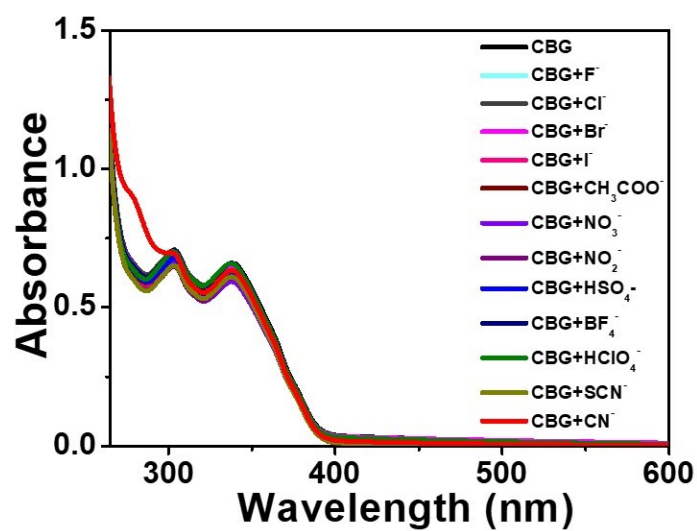


Figure SI-11. Absorption spectra changes upon addition of various anions as their tetra butyl ammonium salts.

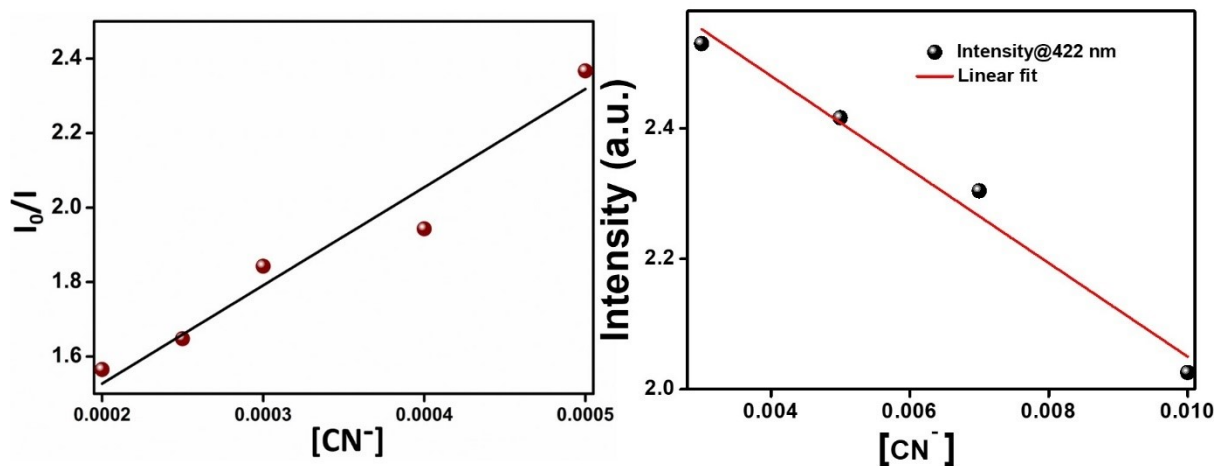


Figure SI-12. a) Stern-Volmer plot of CBG for CN^- sensing and b) determination of detection limit of CBG for CN^- sensing.

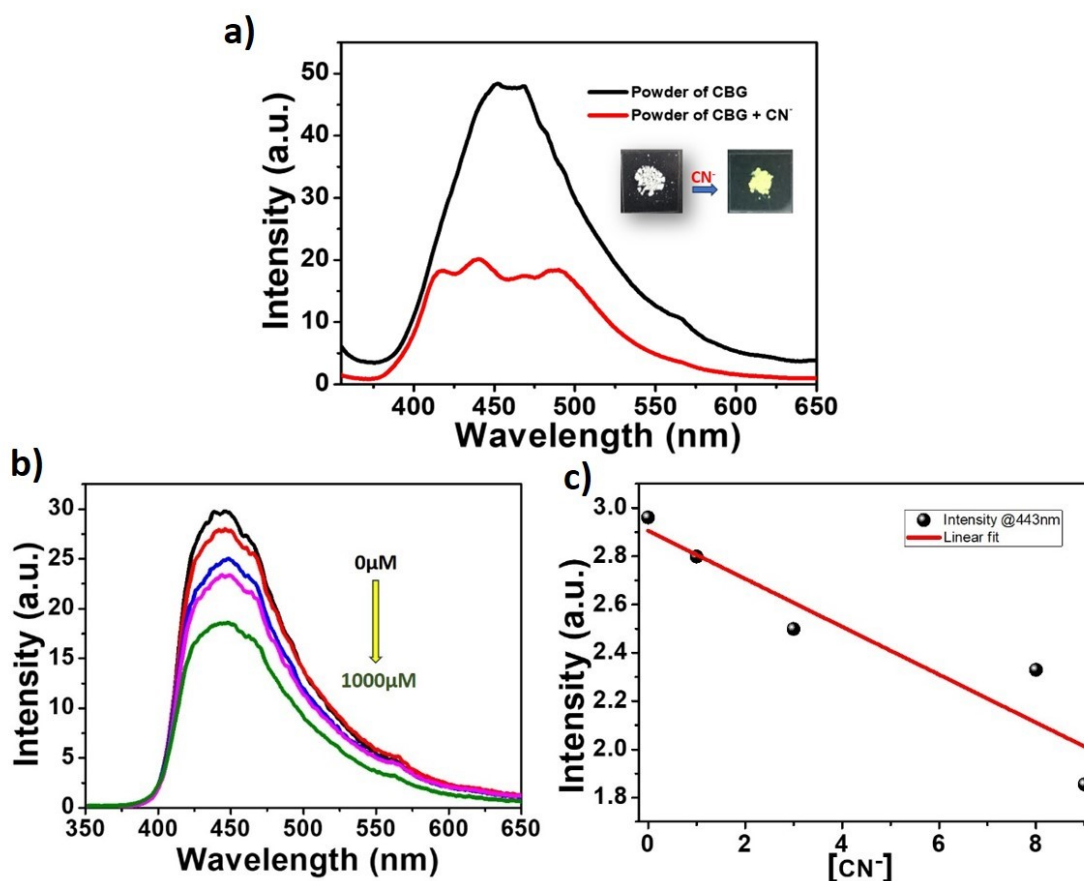


Figure SI-13. a) Emission spectra of CBG in its powder state and after treatment with CN^- b) Decrease in the emission intensity of CBG gel with increase in concentration of aq. CN^- and c) determination of detection limit of CBG gel for CN^- sensing.

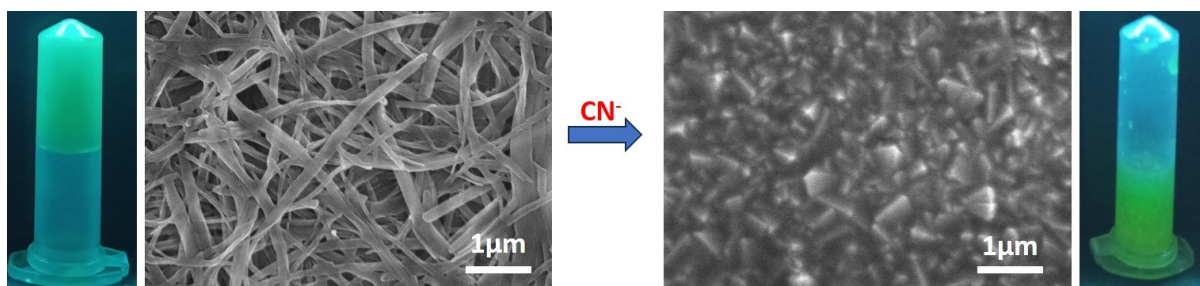


Figure SI-14. SEM image of CBG gel before and after addition on CN^-

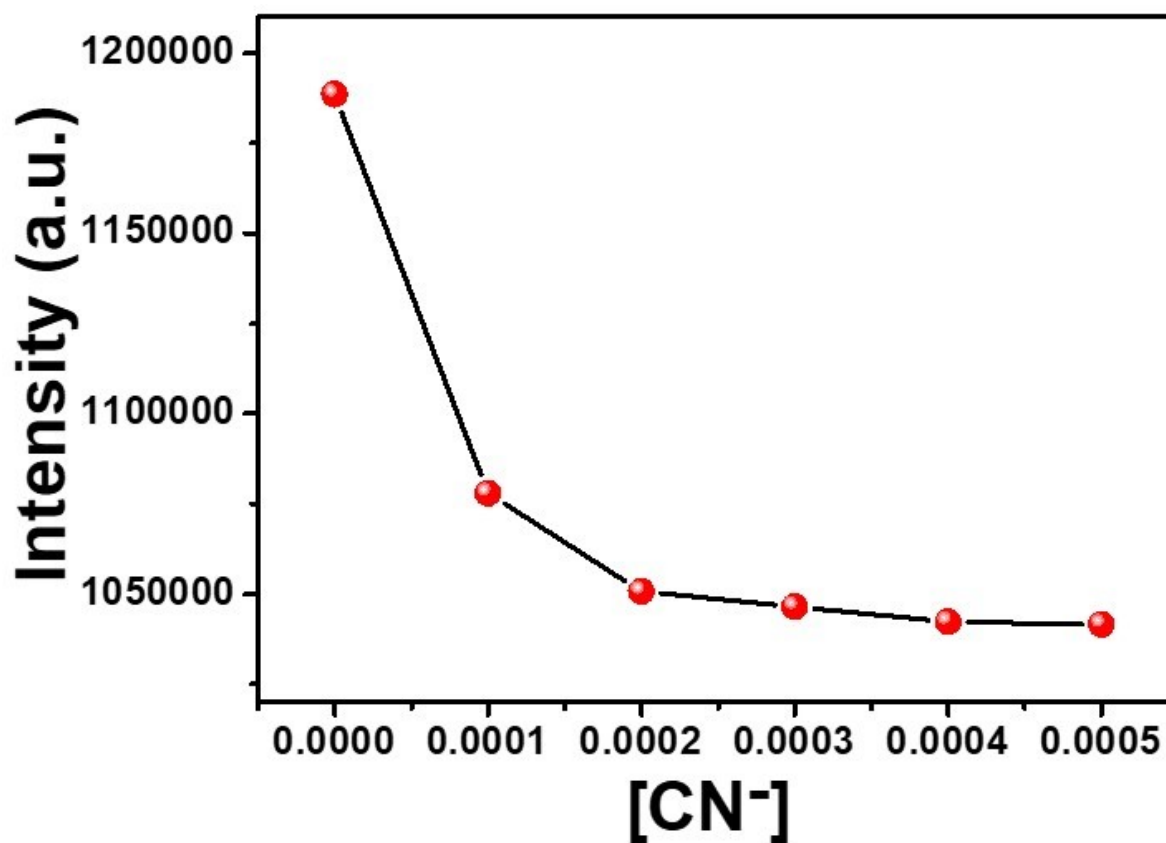
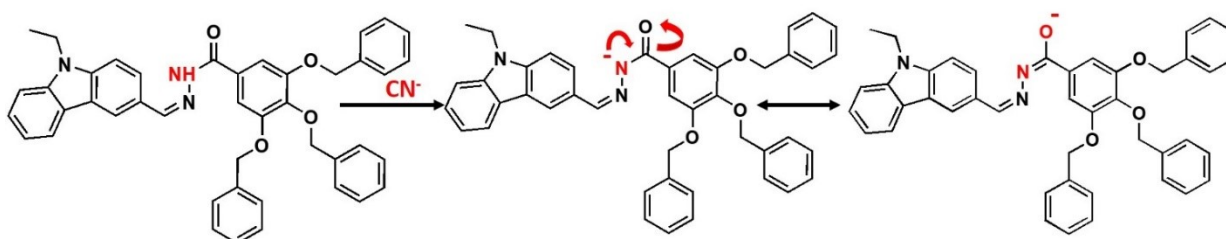


Figure SI-15. Decrease in fluorescence intensity with increase in concentration of CN^- in tap water.



Scheme SI-1. Deprotonation upon cyanide addition followed by the resonance stabilization.

Reference	Detection limit	Medium		
		Solution	Solid	Gel
1	0.28 μ M	Yes	-	-
2	20nM	Yes	-	-
3	67.4 nM	Yes	-	-
4	0.0153 μ M	Yes	-	-
5	51 nM	Yes	-	-
6	11nM	Yes	-	-
7	0.427 μ M	-	Yes	-
8	39.3 nM	Yes	Yes	-
9	0.5 μ M	Yes	Yes	-
10	3.02 μ M	Yes	-	Yes
Present study	1.28nM	Yes	Yes	Yes

Table SI-2. Comparison table of literature reports of cyanide sensing



Figure SI-16. Yellow colour of the solution that appeared at 1.7 V.

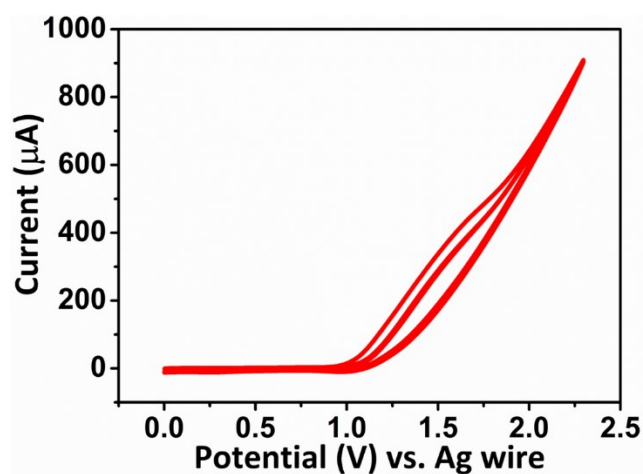


Figure SI-17. CV obtained when FTO plate is used as the working electrode.

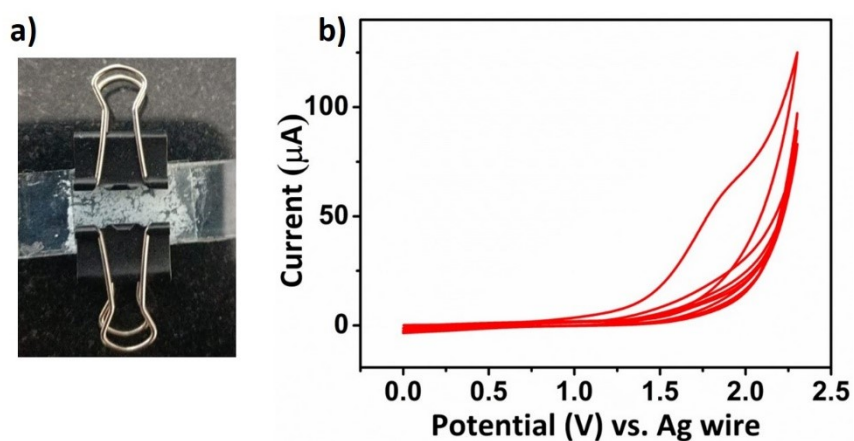


Figure SI-18. a) CBG gel sandwiched between FTO plates and b) CV in gel state.

References

- 1 K. Y. Ryu, J. J. Lee, J. A. Kim, D. Y. Park and C. Kim, *RSC Adv*, 2016, **6**, 16586–16597.
- 2 H. W. Zhao, G. Wu, X. Y. Sun, J. Bin Chao, Y. Q. Li, L. Jiang and H. Han, *J Lumin*, 2018, **201**, 474–478.
- 3 Q. Zou, F. Tao, H. Wu, W. W. Yu, T. Li and Y. Cui, *Dyes Pigm*, 2019, **164**, 165–173.
- 4 J. H. Park, R. Manivannan, P. Jayasudha and Y. A. Son, *J Photochem Photobiol A Chem*, 2020, **397**.
- 5 Z. H. Zheng, Z. K. Li, L. J. Song, Q. W. Wang, Q. F. Huang and L. Yang, *Sensors*, 2017, **17**, 405.
- 6 S. Pramanik, V. Bhalla and M. Kumar, *ACS Appl Mater Interfaces*, 2014, **6**, 5930–5939.
- 7 Z. M. Dong, H. Ren, J. N. Wang and Y. Wang, *Microchemical Journal*, 2020, **397**
- 8 S. Manickam and S. K. Iyer, *RSC Adv*, 2020, **10**, 11791–11799.
- 9 C. Nandhini, P. S. Kumar, K. Poongodi, R. Shanmugapriya and K. P. Elango, *J Mol Liq*, 2021, **327**.
- 10 H. Yao, J. Wang, S. S. Song, Y. Q. Fan, X. W. Guan, Q. Zhou, T. B. Wei, Q. Lin and Y. M. Zhang, *New J Chem*, 2018, **42**, 18059–18065.